One pot microwave synthesis of highly stable AuPd@Pd supported core-shell nanoparticles

Alexander G. R. Howe[1], Peter J. Miedziak[1], David J. Morgan[1], Qian He[1], Peter Strasser[2] and Jennifer K. Edwards[*1]

[1] Cardiff Catalysis Institute, Cardiff University School of Chemistry, Main Building, Park Place, Cardiff, CF10 3AT

[2] Technische Universität Berlin, Fakultät II, Institut für Chemie, Sekretariat TC 3, Straße des 17. Juni 124, 10623 Berlin

[*] Corresponding author edwardsjk@cf.ac.uk

Abstract

A series of 1wt% supported Au, Pd and AuPd nanoalloy catalysts were prepared *via* microwave assisted reduction of $PdCl_2$ and $HAuCl_4$ in a facile, one pot process. The resulting materials showed excellent activity for the direct synthesis of hydrogen peroxide from hydrogen and oxygen, with a synergistic effect observed on the addition of Au into a Pd catalyst. Detailed electron microscopy showed that the bimetallic particles exhibited a core shell morphology, with an Au core surrounded by an Au-Pd shell, with a size between 10-20nm. The presence of Au in the shell was confirmed by EDX studies, with corroborating data from XPS measurements showing a significant contribution of both Au and Pd in the spectra, with the Au signal increasing as the total Au content of the catalyst increased. No PdO was observed, suggesting a complete reduction of the metal chloride nanoparticles. Unlike similar catalysts prepared by sol immobilisation methodology, the core shell structures showed excellent stability during the hydrogen peroxide synthesis reaction, and no catalyst deactivation was observed over 4 reuse cycles. This is the first time the preparation of stable, core-shell particles have been reported using microwave assisted reduction. The observation that these particles are core shell, without the need of a complicated synthesis or high thermal treatment and form in just 15 minutes presents an exciting opportunity for this experimental technique.

Introduction

Mono and bimetallic nano-alloyed particles (NP) anchored to metal oxide or carbon supports are highly efficient, selective catalysts for a wide-ranging number of environmentally friendly reactions, from upgrading biomass to pioneering new reaction pathways to high value commodity chemicals such as hydrogen peroxide.[1,2,3,4,5] The preparation route to these supported nanoparticles has been shown to have a major influence of the activity of the final catalyst, in terms of NP size and composition. Wet impregnation is a simple, scalable preparation method that is commonly reported for bimetallic gold-palladium nanoparticle synthesis that involves the dissolution of metal salts into water, addition of the support and removal of water to form a paste, the final catalyst is formed following oven drying and calcination/reduction. The resulting nanoparticles exhibit a bi-modal particle size distribution, with some smaller particles (2-8nm) present but where a significant amount of the metal is tied up in large metal particles (50-1000nm), which reduces the total metal surface area. [5] Hutchings *et al.* have shown that there is also a composition variation within these particles, where the smaller particles are palladium rich and the larger particles are gold rich.[6] Deposition precipitation is another widely reported preparation method, where desired precipitation of specific metal complexes is achieved by pH adjustment, these then adhere to the catalyst support (chosen based on isoelectric point) through electrostatic bonding. Nanoparticles synthesised during this process have a much smaller average particle size (2-6nm), however this technique requires the use of extremely dilute metal salts, (e.g. 150 ml g^{-1}), which makes this process difficult to scale to an industrial level as it requires copious filtration (and washing) to obtain the final catalyst.[7] Furthermore, not all the metal is deposited on the support leading to loss of precious metals or additional recovery steps that would incur additional costs. The co-precipitation method has also been reported for the preparation of bi-metallic nanoparticles where the support is precipitated at the same time as the desired metal complex. In this method some of the active metal can be lost inside the lattice of the support and this technique also suffers from the same disadvantages as the deposition precipitation method.[8]

In recent years the sol-immobilisation method has been developed where the addition of aqueous metal salts to polymeric capping agents, followed by reduction with $NaBH_4$ h provides metal nanoparticles with exceptionally narrow (2-4nm) size distribution and with fine control over the final structure (core-shells are produced when consecutive reduction of the metal salts occurs, random homogeneous alloys are formed when both metal precursors are added at the same time).[9,10] However the capping polymers can inhibit access to the active metal particles, which either results in a lower rate of reaction or the need for additional

procedures to remove the polymer, such as calcination or reflux. This technique also requires a high volume of solvents (e.g. 400 ml g^{-1}) and the composition of the nanoparticles is dependent on their size, so accurate determination of the active alloy composition is impossible.[7]

The formation of core-shell nanoparticles presents a particular challenge in catalyst preparation. Core-shell nanoparticle catalysts afford the improved catalytic performance of alloyed bimetallic catalysts, whilst allowing their properties to be further optimised through variation of the core diameter and shell thickness.[11,12,13] The preparation of core-shell nanoparticle catalysts typically requires careful refinement of methods used to prepare alloyed bimetallic catalysts. In the case of AuPd/TiO_2 catalysts prepared by impregnation for alcohol oxidation, it was found that subjecting the catalyst to a specific heat treatment regime resulted in Pd segregation to afford core-shell particles. These core-shell particles exhibited significantly improved activity versus monometallic catalysts subjected to the same calcination protocol.[14] Core-shell nanoparticle catalysts can also be prepared by sol immobilisation. It has been found previously that supported Au core-Pd shell nanoparticle catalysts can be prepared through the sequential reduction of gold and metal precursors using sodium borohydride.[15] Whilst the Au@Pd and Pd@Au catalysts offer unique selectivity and activity improvements over alloyed catalysts, this comes at the cost of an increasingly complex and elaborate preparation protocol. The presence of small (<3nm) monometallic particles in core-shell catalysts indicates that a portion of the metal remains in the relatively inactive segregated state, reducing catalyst efficiency.

Another preparation method that relieves heavily on NP synthesis through reduction in aqueous solution is the so-called polyol method, a solution phase preparation technique in which metal precursors are reduced by a reductive species formed from the (typically) polyol solvent at elevated temperatures.[16] The versatility of this method is evident from the variety of mono-metallic nanoparticles reported to be prepared in this way – Ag, Au, Pd, Pt, Fe, Ni, Co and Sn to name a few.[17,18,19] The polyol method has also been refined to prepare bimetallic nanoparticles, the well controlled growth kinetics have allowed it to be used to prepare materials with specific magnetic and crystallographic properties.[20] A wide range of alcohol solvents are suitable for solvent reduction in addition to other species such as N,N-Dimethylformamide (DMF).[21] The properties of DMF are sufficiently similar to polyols (high boiling, polar and forms reductive species) such that it can be easily substituted to prepare a variety of metal nanoparticles, most notably silver.[22]

DMF has been found to be particularly useful in the preparation of core-shell nanoparticles of varying composition. Tsuji and co-workers found that the choice of solvent was critical in the preparation of Au@Ag core-shell nanocrystals. It was found that reduction in DMF lead to the formation of highly faceted icosahedral core-shell particles, which was not observed for preparations in ethylene glycol.[23] The versatility of DMF as solvent and reductant for core-shell particle preparation is attributed to the variable reduction rate of metal precursors in DMF. It has been found that Ag^{+} and Au^{3+} species reduce rapidly in DMF at temperatures as low as 25°C.[24,25] A comparison of clay supported Ni and Ag nanoparticles found that solvent reduction of pre-impregnated metal precursors resulted in smaller Ag^{0} nanoparticles (<5nm) versus the Ni containing material (15-20nm). This was found to be a consequence of the reduction rate of the different precursors with faster seed formation resulting in smaller Ag particles.[26] Solvent reduction in DMF therefore offers a convenient method to prepare core-shell nanoparticle catalysts whilst avoiding sequential reduction, and therefore extraneous monometallic species.

Microwave heating is a technique that offers significant advantages over conventional heating – especially in the field of nanoparticle synthesis. Principally, microwave irradiation affords uniform internal heating of the preparation resulting in facile nucleation and crystallisation.[27] Other benefits include faster temperature ramping (temperatures as 150 ^{o}C – 250^{o}C can be achieved in less than 1 minute, compared to over 30 minutes for conventional heating), a lack of convection processes and convenience. A comparison of Rh nanoparticles prepared by solvent reduction using microwave and conventional heating found that the microwave processed catalysts exhibited a two-fold increase in activity for cyclohexene hydrogenation, compared to those prepared by conventional heating. This difference was ascribed to improved nanoparticle morphology and size control. It was found that microwave prepared catalysts exhibited predominantly tetrahedral particles of 5-7nm diameter, whilst the conventionally prepared catalysts displayed particles of varying morphology and size.[28]

One reaction in which highly dispersed bimetallic Au-Pd nanoparticles are known to show exceptionally high activity is the direct synthesis of hydrogen peroxide from molecular hydrogen and oxygen. Hydrogen peroxide is a major commodity chemical and is considered to be a green oxidant as the only by-product from the oxidation is water It can be used as an alternative to stoichiometric oxygen donors, such as chromates and percarbonates, which have associated toxicity issues.[29,30] Hydrogen peroxide is currently produced by the anthraquinone cycle, a process only economical when carried out on a large scale, which produces highly

concentrated hydrogen peroxide after a distillation process. This concentrated hydrogen peroxide often requires significant dilution at the point of use, therefore a direct process, where dilute streams of H_2O_2 can be produced on site at the point of use, would be desirable.

The earliest reports used palladium as the catalyst and more recent work found that gold supported on alumina, could be an effective catalyst for the direct synthesis reaction.[31,32] A significant improvement in the activities came upon the discovery that alloying gold and palladium led to much higher H_2O_2 synthesis rates.[32] The additional activity of these catalysts was attributed to better hydrogen selectivity for an AuPd catalyst system compared to a Pd only system. Further studies showed that alumina supported catalysts were core shell in nature, with a Pd rich shell surrounding an Au rich core.[33] Subsequent work has looked at different supports for bimetallic nanoparticles, Edwards *et al.* reported that core shell structureas were also observed when iron oxide was used as a support.[34] Subsequent work by Ishihara *et al.* studied gold supported on a range of oxides and zeolites, they also reported an improvement in the rate of peroxide formation upon the addition of palladium to gold.[35] Hutchings *et al.* reported that titania, different gold to palladium ratios were tested, however the 1:1 ratio was found to be the optimum. In the same work the authors investigated the effect of calcination temperature, uncalcined catalysts were found to be the most active, followed by those calcined at 200 °C and then those calcined at 400 °C, however the stability of these catalysts followed the opposite trend to the activity.[5]

In this work, we have synthesised monometallic and bimetallic gold palladium catalysts using a microwave assisted reduction synthesis method, we have found that catalysts can be quickly and easily prepared by this method and have excellent activity for hydrogen peroxide synthesis. The catalyst exhibit core shell structures where a gold rich core is surrounded by a Pd rich (but with a tangible Au component) shell. This type of core shell particle is one of the first instances where the Au in the disruption of a Pd surface has been directly imaged, corresponding to greater catalytic rates, and aligns with previous theoretical studies.[36,37]

Experimental

Catalyst preparation

1wt%Pd, 1wt%Au and bimetallic AuPd catalysts were prepared using a CEM Discover SP microwave reactor. TiO_2 (P25, Degussa) was used as the support. Aqueous stock solutions of $PdCl_2$ (Sigma Aldrich) and $HAuCl_4$ (STREM Chemicals) were prepared in 0.2M HCl. The stock solutions were of concentrations 15mg/mL and 12.5mg/mL Pd and Au respectively. The

0.5%Pd0.5%Au/TiO_2 catalyst was prepared as described below. TiO_2 was added to the quartz microwave reaction vessel, followed by the addition of $PdCl_2$ solution (83µL) and $HAuCl_4$ (102µL), and DMF (2.8mL). The mixture then underwent a microwave treatment, heating to 150°C in 1 minute, followed by holding at this temperature for 15 minutes. The catalyst preparation was stirred at 1200rpm throughout using a magnetic stirrer. The microwave reactor was operated in isothermal mode, with microwave power and pressure varying between 0-200W and 0-3 bar respectively. The mixture was cooled, filtered, and washed using 20mL 4:1 water: ethanol. The resultant catalyst was dried at 110°C for 16h before use.

An analogous 0.5%Pd0.5%Au/TiO_2 catalyst was also prepared using conventional heating. Briefly, $PdCl_2$ (83µL) and $HAuCl_4$ (102µL) stock solutions were added to 0.25g TiO2 and 2.8mL DMF in a round bottle flask. The flask was submerged in an oil bath heated to 150°C, and stirred at 1200rpm for 2 hours. The preparation mixture was then cooled and washed with 20mL 4:1 water:ethanol before being dried at 110C for 16hr before use.Catalysts of composition 0.2%Pd0.8%Au, 0.25%Pd0.75%Au, 0.33%Pd0.66%Au, 0.5%Pd0.5%Au, 0.66%Pd0.33%Au, 0.75%Pd0.25%Au, 0.8%Pd0.2% and 1%Pd and 1%Au were prepared using this method

Catalyst Evaluation

Catalysts were tested for their direct hydrogen peroxide synthesis and hydrogenation activity using a stainless-steel autoclave (Parr). The 100mL autoclave was fitted with a Teflon liner – nominal volume 66mL. In a typical synthesis test, the autoclave was charged with catalyst (0.01g), water (2.9g) and methanol (5.6g), then purged with 5%H_2/CO_2 three times before being filled with 5%H_2/CO_2 (29 bar) then 25%O_2/CO_2 (11 bar). The autoclave was chilled to 2°C before stirring at 1200rpm for 30min.

Catalysts were tested for hydrogen peroxide hydrogenation activity in a similar manner. In this case the Teflon liner was charged with 50% hydrogen peroxide solution (0.68g), water (2.22g) and methanol (5.6g) to yield a 4wt% hydrogen peroxide solution, followed by the addition of catalyst (0.01g). The autoclave was purged with 5%H_2/CO_2 three times before being filled with 5%H_2/CO_2 (29 bar). The autoclave was chilled to 2°C before stirring at 1200rpm for 30min.

In both cases the hydrogen peroxide content of the solutions was determined by titration of small aliquots of the filtered reaction solution with cerium sulphate ($CeSO_4$) in the presence of ferroin indicator solution.

Catalyst reuse was also investigated. The catalyst (50mg) was collected post synthesis reaction, filtered, washed thoroughly with water and acetone and dried for 16hr at 110 °C. The synthesis activity of this used catalyst was evaluated using the procedure outlined above.

Characterisation

Microwave plasma atomic emission spectroscopy (MP-AES). Catalyst metal loadings were determined using an Agilent 4100 MP-AES (Microwave Plasma Atomic Emmision Spectrometer).

Briefly, 25mg of catalyst sample was digested in 20% aqua regia for 24h following filtration prior to analysis. The white TiO_2 was removed by filtration. Quantification of the catalyst metal loadings in the filtrate was determined by emission intensity at multiple wavelengths, 242.795 and 267.595nm for Au and 340.458 and 363.470nm for Pd respectively. The emission intensity was calibrated using certified Au and Pd reference solutions (Agilent), in all cases $r^2 > 0.999$

X-ray photoelectron spectroscopy (XPS) data was collected on a Thermo-Fisher Scientific K-Alpha$^+$ X-ray photoelectron spectrometer using a monochromatic Al Kα X-ray source operating at 72 W. Survey scans and high-resolution scans were acquired at a pass energy of 150eV and 40eV respectively. Charge neutralization was achieved using a combination of low energy electrons and argon ions, resulting in a C(1s) binding energy of 284.8 eV; experimental binding energies are quoted ±0.2 eV

The Scanning Transmission Electron Microscopy (STEM) images and X-ray Energy Dispersive Spectra (X-EDS) were taken using a JEOL® JEM-ARM200F aberration corrected microscope, equipped with an Oxford Instrument® Aztec EDS system.

Results and Discussion

Effect of Catalyst Composition on Hydrogen Peroxide Synthesis Activity

Initially, monometallic catalyst were prepared along with a series of catalysts where the gold-palladium ratios were varied in the range 0.2-0.8wt%Pd. It has previously been found that for catalysts prepared by a multiple preparation methods, including wet impregnation and sol-immobilisation that the optimum gold palladium ratio is around 1:1 by mass. Compositions

that are either richer or leaner in palladium exhibited reduced hydrogen peroxide synthesis activity.[5,38,39]

The synthesis and hydrogenation activities of the microwave prepared catalysts are shown in Figure 1. In agreement with the work that has been reported previously using catalysts prepared by other methods, a synergistic effect is observed on addition on incorporation of a small amount of Au into a Pd catalyst. The monometallic Au and Pd catalysts had activities of 5 and 35 $molkg_{cat}^{-1}h^{-1}$.[40] However, unlike the previous work, the catalyst activity does not display a 'volcano' trend, with 0.5%Pd0.5%Au/TiO_2 not being the most active catalyst as would be expected with other preparation methods. Instead the highest rates of hydrogen peroxide synthesis, 80 $molkg_{cat}^{-1}h^{-1}$ and 76 $molkg_{cat}^{-1}h^{-1}$ were observed in the most palladium rich bimetallic catalysts, 0.8%Pd0.2%Au/TiO_2 and 0.75%Pd0.25%Au. The activity of every bimetallic catalyst was higher than the monometallic Pd analogue, indicating the positive contribution of Au, however reducing the palladium content below 0.66% has a less marked effect on the resulting activity. This suggests that the ideal composition of a metal particle is quite palladium rich, with only a small amount of gold required to provide the positive effect. The gold must have a role in the active site as the monometallic palladium catalyst is significantly less active than any of the bimetallic catalysts. The fact that there is only a small reduction in activity of the catalyst between palladium contents of 0.7 and 0.2 suggests that although the gold is playing an important role in the active species, not a lot of it is required and therefore it is possible that in the catalysts with higher gold content some of the gold is present in an inactive, spectator form.

Catalysts were also evaluated for hydrogen peroxide hydrogenation activity. Over hydrogenation of hydrogen peroxide is the principle decomposition pathway of hydrogen peroxide produced by catalytic direct synthesis.[41] The hydrogenation activity was found to vary with catalyst composition, but with no discernible trend. All catalysts exhibited hydrogen peroxide hydrogenation activity in the region of 100-200 $molkg_{cat}^{-1}h^{-1}$. These hydrogenation activities are nonetheless considerably lower than those previously reported for other preparation methods (figure 1), indicating that catalysts prepared by this solvent reduction method are significantly more selective towards hydrogen peroxide over water.[42,43] A catalyst of composition 0.5%Pd0.5%Au/TiO_2 prepared by sol immobilisation has previously been found to have twice the hydrogenation and an accompanying decrease in synthesis activity relative to the analogous catalyst we report here, as shown in figure 1.[15,44]

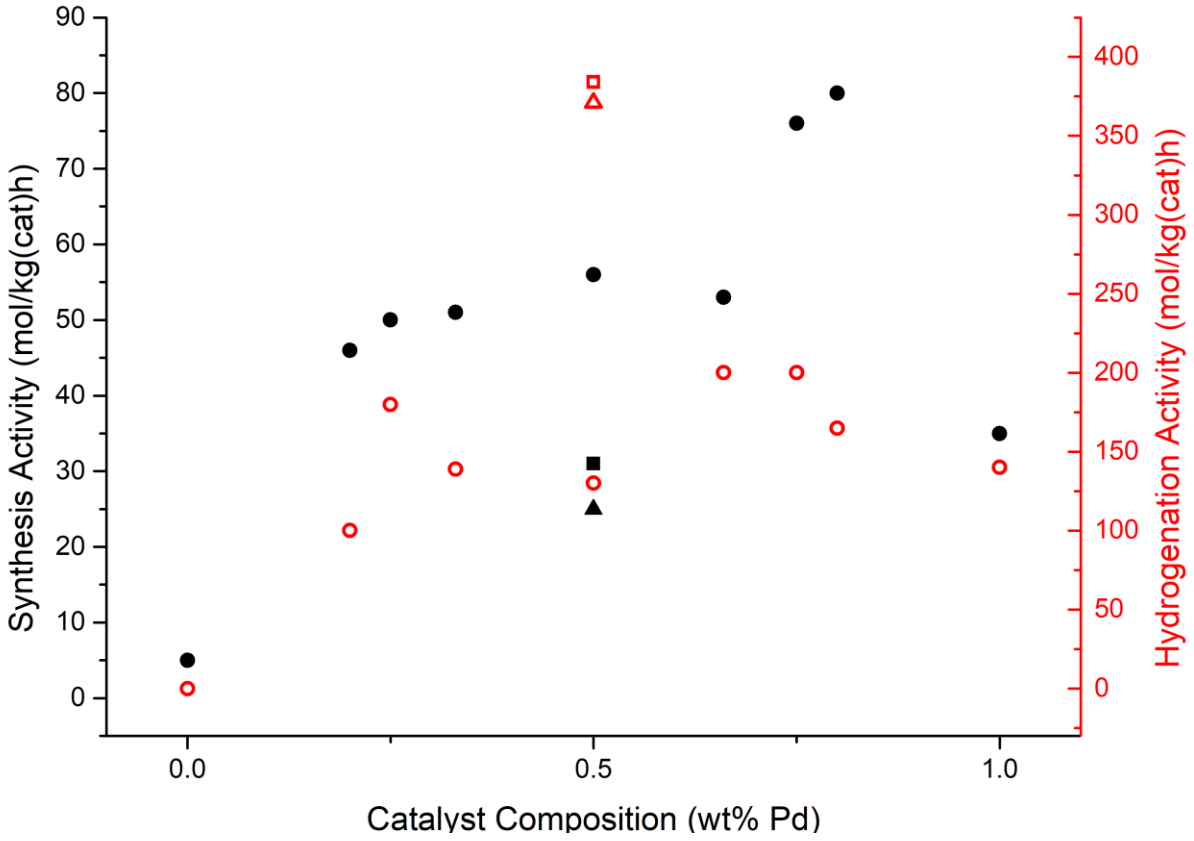

Figure 1: The hydrogen peroxide synthesis activity (closed symbols) and hydrogen peroxide hydrogenation activity (red open symbols) for the microwave catalysts (●○) prepared with varying palladium and gold compositions. The activity for a 1%0.5Au0.5Pd/TiO_2 random alloyed Au+Pd(■□) and Pd@Au (▲△) core-shell sol immobilisation catalyst are included from reference ([44]).

For the heritage catalysts prepared by sol immobilisation, the optimum concentration of AuPd was 50/50 by weight, and resulted in the highest activity for H_2O_2 synthesis, both for core-shell (25 $molkg_{cat}^{-1}h^{-1}$) and random alloyed (32 $molkg_{cat}^{-1}h^{-1}$) particles.[44] Interesting the activity of the microwave prepared catalyst was much higher (56 $molkg_{cat}^{-1}h^{-1}$) in terms of H_2O_2 synthesis activity, but the hydrogenation activity (150 $molkg_{cat}^{-1}h^{-1}$) of the microwave prepared catalyst is much lower than that of the sol immobilisation catalysts (375 and 380 $molkg_{cat}^{-1}h^{-1}$) for a nanoparticles with identical loading, immobilised on the same support. This suggests that the microstructure of the surface of the catalyst prepared using microwave reduction is much more selective that that of the sol immobilised nanoparticles. For comparison purposes, an analogous 0.5%Au0.5%Pd/TiO_2 catalyst was prepared using conventional hotplate heating to 150 ^oC. The resulting catalyst showed a visible inhomogeneous distribution of metals, with patches of white, bare titania observed. The catalyst shows much lower activity for the direct synthesis reaction (30mol $molkg_{cat}^{-1}h^{-1}$) and lost 30% of its activity after one use, so was not studied further.

Effect of Total Metal Loading on Turnover

Catalysts were also prepared with varied total metal loading (0.25-1wt%), whilst maintaining a constant Pd:Au mass ratio of 1, in order to investigate the relative dispersion of the metals. It was found that decreasing the metal content results in an equivalent decrease in hydrogen peroxide synthesis activity such that the turn-over frequencies of the catalysts remain roughly constant. This is unusual for bimetallic catalysts prepared by any of the methods described previously, and suggests that the active site, whatever that may be, does not agglomerate or interact with any neighbours as the metal loading is increased. The addition of extra metal seems to simply form proportionally more of the active component, rather than forming different, less active microstructures. These active components either do not interact with each other or are sufficiently separated on the catalyst that the increased number of them does not cause deactivation. This suggests that this preparation method is highly scalable and the catalysts could be tuned to have a large amount of support, to minimise the amount of precious metal required or use a high metal loading to minimise the catalyst amount, as is required by the process. Indeed, it has been reported in the literature that this type of microwave preparation can be used to obtain a highly dispersed 50wt%Pt catalyst. It was found that the 50%wt%Pt/C catalyst displayed nanoparticles with an average diameter of 2.7nm and superior performance against a benchmark commercial catalyst for the oxygen reduction reaction.[45] It should be noted that we base the turnover on the total number of moles of Pd present in the catalyst, as we were unable to quantify the specific Pd metal surface area. Hence the numbers should be used for (catalyst) comparison purposes (to new and heritage data), and to identify trends in the current data as opposed to being absolute figures.

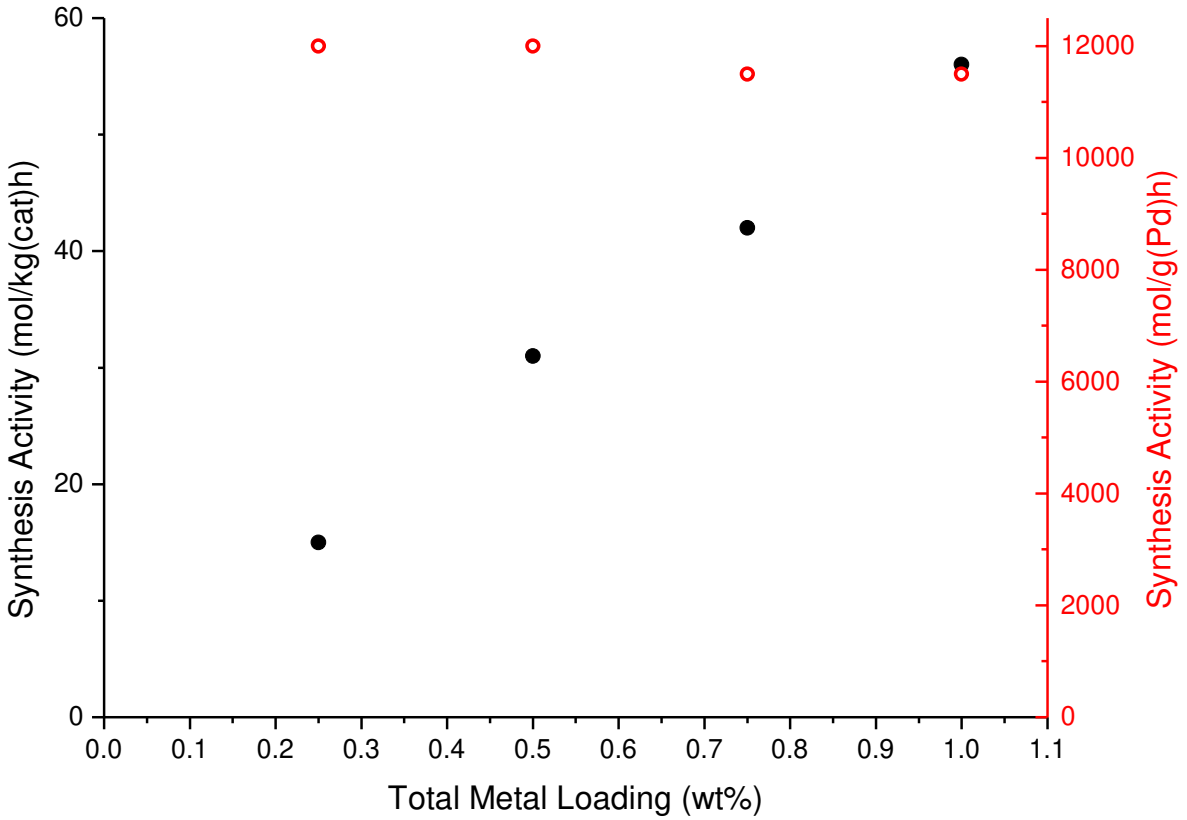

Figure 2: The hydrogen peroxide synthesis activity (●) and hydrogen peroxide hydrogenation activity (○) for the catalysts prepared with varying palladium and gold compositions.

Catalyst Reusability

Catalyst reusability is a vital parameter for precious metal containing catalysts. In the case of direct hydrogen peroxide synthesis, unstable catalysts can leach precious metals into the reaction mixture, resulting in catalyst deactivation or the formation of catalytically active, but inseparable homogenous moieties. The hydrogen peroxide synthesis activity of the catalyst after first, second and third reuses is shown in Figure 3. Synthesis activity decreases by less than 5% upon catalyst reuse. This value is within experimental error indicating that the catalyst is stable. This is a considerable advantage to catalysts prepared using this method, over other colloidal methods such as sol-immobilisation.[46] The effect of heat treatment on AuPd catalysts prepared by sol immobilisation has been previously explored in an attempt to prepare reusable catalysts.[47] It was found that the calcination of catalyst samples resulted in a decrease in hydrogen peroxide synthesis activity and did not afford a strong metal-support interaction such that the catalyst was reusable without appreciable deactivation.[48]

This also contrasts to catalysts prepared wet impregnation, which require heat treatment at considerably harsher temperatures (400 ^{o}C) in order to retain catalyst activity upon reuse.[5]

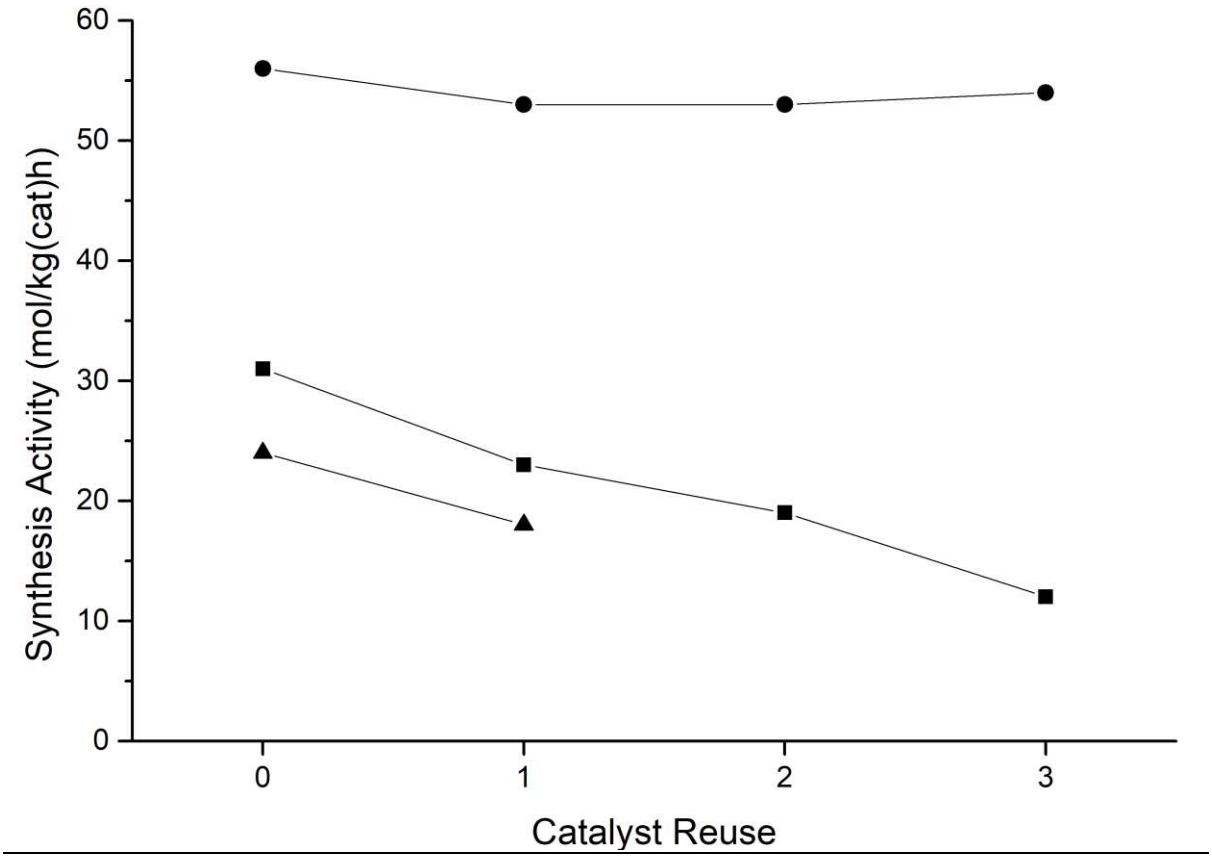

Figure 3: Hydrogen peroxide synthesis activity for the 0.5Au-0.5Pd/TiO_2 catalyst prepared by Microwave heating (●), Au+Pd sol immobilisation (■) and Pd@Au sol immobilisation (▲) over several reuse cycles. Au+Pd and Pd@Au values reproduced from (36).

Catalyst Characterisation

Given the excellent activity and stability of these catalysts, and that there are no literature examples of supported AuPd bimetallic catalysts prepared using this methodology, we were keen to undertake detailed microscopic and spectroscopic analysis of the catalysts, in order to see the fine chemical structure and how this compares to nanoparticles formed using other preparation techniques.

Scanning Transmission Electron Microscopy

Initially we decided to study these materials using aberration corrected scanning transmission electron microscopy (STEM) in order to determine the microstructure of the nanoparticles. We have successfully utilised this technique before to identify small and large core-shell and random alloy AuPd structures.[34,15] Representative STEM high angle annular dark field (HAADF) images of the monometallic Pd/TiO_2 catalyst and the bimetallic 0.5Au-0.5Pd/TiO_2 catalysts are shown in Figure 4. In the HAADF images, precious metal particles, such as Au or Pd, can be easily distinguished from TiO_2 support particles due to their higher atomic numbers. For the same reason Au (Z=79) can also be distinguished from Pd (Z=46). Therefore, the HAADF imaging can provide both structural and chemical information of the catalyst. From Figure 4 (a) and (c), it can be seen that in both catalysts, 10-20 nm metal particles can be found, which are highlighted using dashed white circles. Given the low loading of Au and Pd (1wt%) and the size of the (particles 10-20 nm), it was not possible to acquire enough information to obtain a statistically valid particle size distribution (PSD). The particles obtained using this methodology are slightly larger than those we observe when the catalysts are prepared by the sol immobilisation method, however, the activity data discussed previously demonstrates that these particles are catalytically active for this reaction. Furthermore, as the hydrogenation activity is significantly lower than when the catalyst is prepared by the sol immobilisation method, suggesting that the hydrogenation occurs at a higher rate on small metal nanoparticles, given the higher surface area of particles with a smaller volume. The higher magnification images of the individual particles for the two catalysts are shown in Figure 4 (b) and (d), respectively. We were surprised to observe that the bimetallic 0.5Au-0.5Pd/TiO_2 catalyst possessed a distinct core-shell morphology. The particle shell is rich in Pd and therefore has a

lower intensity compared to the core, which is rich in Au. The shell is not likely to be pure Pd, however, as there are higher intensity regions as highlighted by the arrow in the Figure 4(d).

Clearer evidence of the core-shell morphology for the particles in the bimetallic 0.5Au-0.5Pd/TiO_2 catalyst can be found using STEM X-ray energy dispersive spectroscopy (X-EDS). The STEM HAADF image, and the corresponding X-EDS chemical maps obtained from the spectrum images of Au (green) and Pd (red) are shown in Figure 5. The Au-rich core and Pd-rich shell morphology shown in the X-EDS maps is consistent with the HAADF images. Spectra from the shell (area A) and the core (area B) can also be extracted from the spectrum image and are also shown in Figure 5. It can be seen that the Au M peaks can still be found from the particle shell, and it is relatively lower compared to that from the particle core. This is in agreement with the experimental data discussed earlier, and the bi-metallic nature of the shell and largely monometallic nature of the core could explain the relatively small differences in activity between the catalysts prepared with gold and palladium in different ratios, it is possible that the shell is always bi-metallic and the difference in the amount of gold in the catalyst changes the size of the core and has no influence on the shell composition. We cannot however confirm this without a further detailed HR-TEM study.

Au-Pd core shell particles has previously been observed in catalysts prepared by both wet impregnation and sol-immobilization.[14,15] In the case of the wet impregnation, core-shell morphologies are believed to be formed during the calcination treatment, while the Pd diffuses out due to a higher oxygen affinity, and possibly forms a thin layer of oxide. In the case of sol-immobilization, excess and strong reductant is usually used (e.g. $NaBH_4$) and therefore Au and Pd are both quickly reduced regardless of their difference in the reduction potential. The formation of the core-shell morphology using the sol-immobilization method therefore can be controlled by the sequence of the reduction.[15]

In the current case, the formation of the particles with Pd-rich shell and Au-rich core morphologies in the 0.5Au-0.5Pd/TiO_2 suggested that the particle formation is likely to be controlled by the reduction potential of the two elements, with the Au reducing first and possibly forming a seed onto which the Pd deposits, with some remaining Au in solution then incorporating into the Pd shell as it forms. This is consistent with previous work on the preparation of Au and Pd nanoparticles using solvent reduction in DMF. It has been observed that Au^{3+} ions reduce readily to Au^{+} then Au^{0} at temperatures as low as room temperature, with rates increasing significantly at temperatures above 150°C.[22] Additionally, a study of Pd

nanoparticles prepared from the solvent reduction of glycerol found that nanoparticles to be highly anisotropic and of varying morphology, a consequence of the comparatively slower reduction kinetics.[49] Interestingly, clear evidence of the presence of Au in the Pd shell is observed by STEM HAADF imaging, X-EDS mapping and XPS, which is consistent with the synergistic effect between the two elements in terms of the catalytic activity towards hydrogen peroxide synthesis.

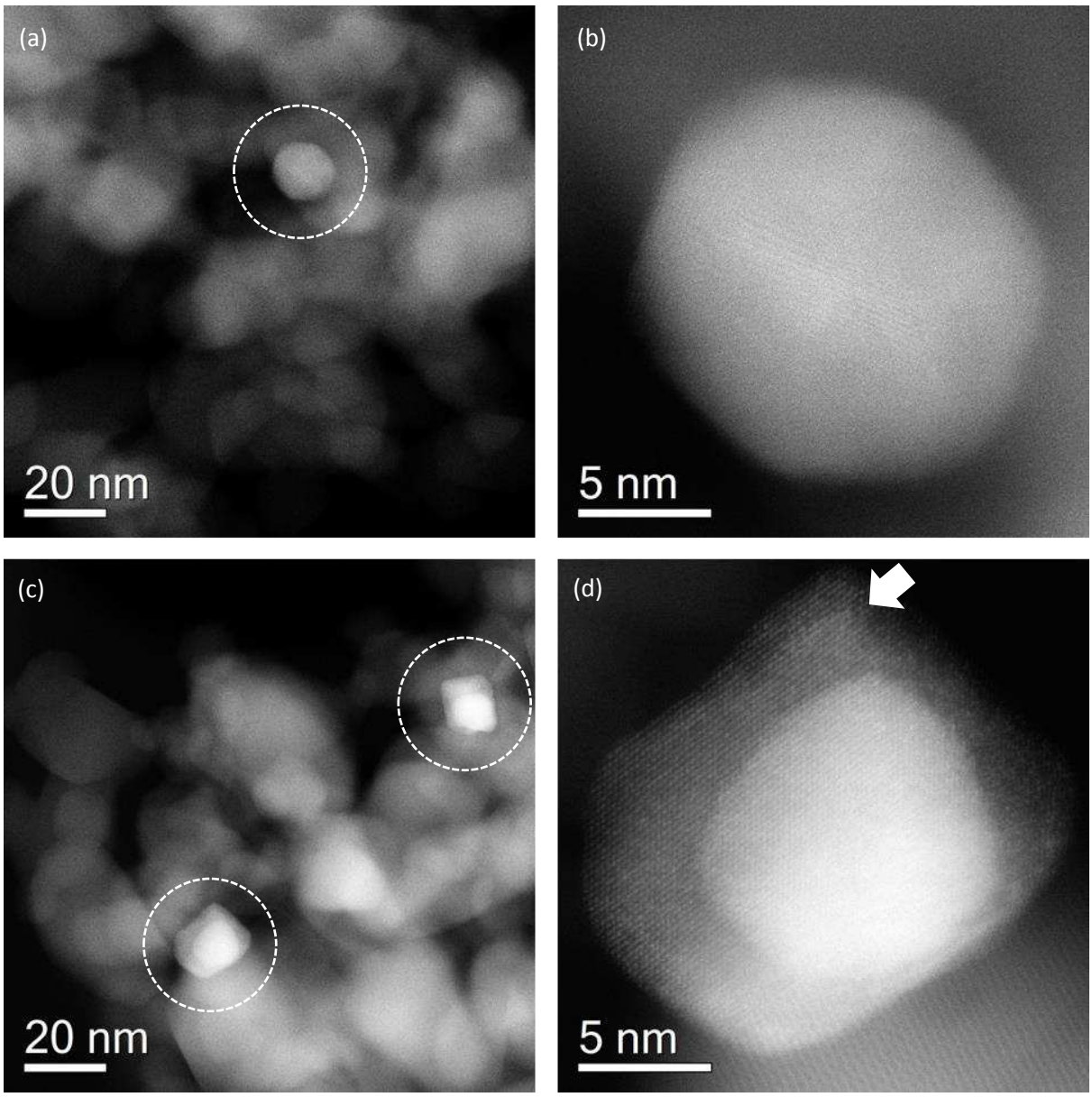

Figure 4. Representative STEM-HAADF images of (a, b) Pd/TiO_2 and (c, d) $0.5Au\text{-}0.5Pd/TiO_2$ catalysts. In (a) and (c), metal particles (highlighted in dashed circles) can be distinguished from the

TiO_2 support particles due to higher intensities. A core-shell structure can be found in the 0.5Au-0.5Pd/TiO_2 catalyst. White arrow in *(d)* highlights the possible presence of Au in the apparent Pd-rich shell.

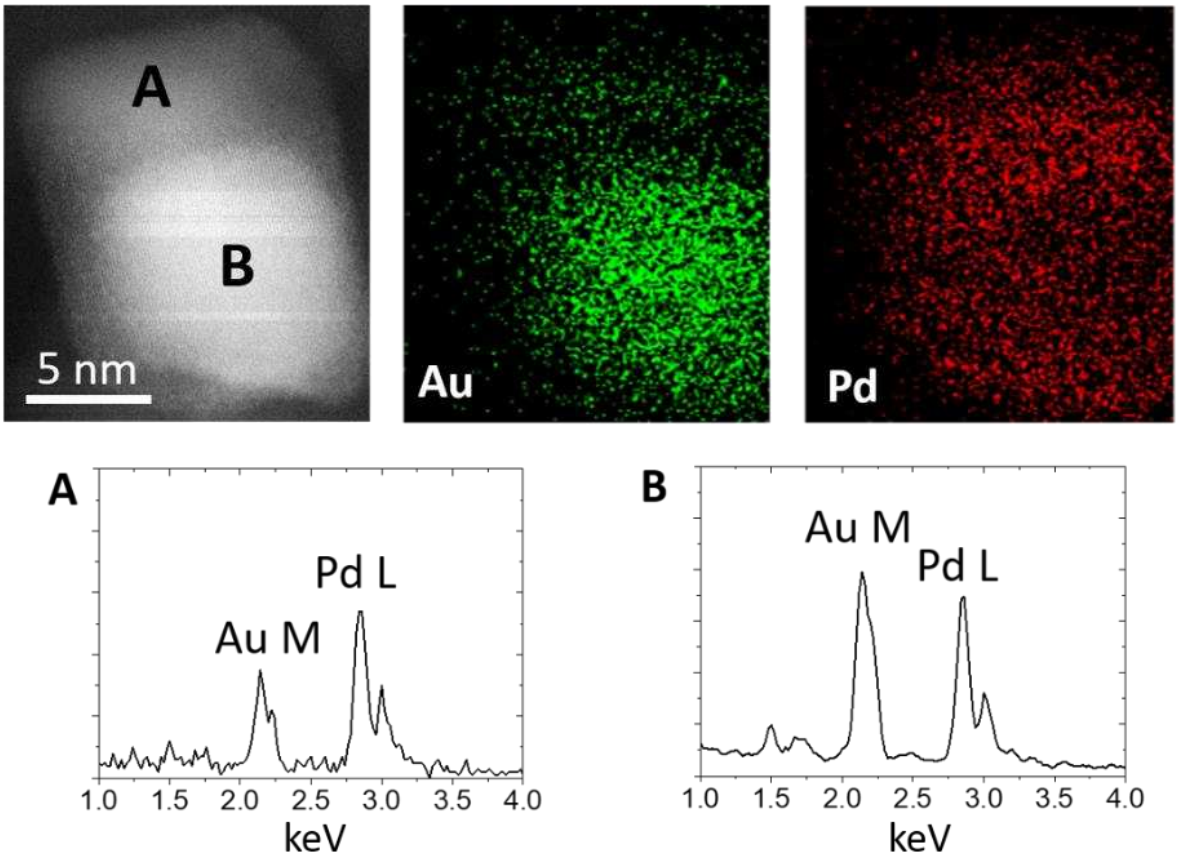

Figure 5. Representative STEM-HAADF image, and the corresponding X-EDS analysis of the 0.5Au-0.5Pd/TiO_2 catalyst. The Au and Pd maps are shown in green and red respectively, confirming the core-shell structure of the particle. The spectra from area A and B are shown, confirming the presence of Au in the apparent Pd-rich shell.

X-Ray Photoelectron Spectroscopy (XPS)

XPS is a surface sensitive technique that is used to give a chemical fingerprint of a catalyst surface. Analysis of the Au-Pd/TiO_2 catalysts reveal Au($4f_{7/2}$) and Pd($3d_{5/2}$) binding energies of 83.4 and 334.9 eV respectively; no Pd(II) species were observed for any of the catalysts, including the monometallic Pd/TiO_2 indicating the reductive treatment of the nanoparticles in the microwave was sufficient to reduce all of the metal. The low binding energy of the Au(4f) signal is has been previously ascribed to charge transfer between Au and reduced TiO_2 surfaces, hydrogen treatment and the lower coordination of small Au particles .[50,43] Based on the

electronegativity of the two metals and in agreement with the findings of Lee et al., any charge transfer would be negligible, therefore we attribute to low binding energy to the low coordination of the Au atoms in the core. Such an interpretation would be consistent with microscopy results [51]

It is clear from the Pd(3d)/Au(4d) spectra (Figure 6), that as the amount of Pd in the catalyst increases, the Au signal decreases, consistent with an increasing Pd shell thickness. The tabulated results are given in table 1.

Table 1 . Tabulated at% surface concentration of Au, Pd, Ti, O and C on 1wt% AuPd/TiO_2 catalysts with varying Au:Pd ratios. XPS spectra are quantified using the integrated peak areas, after subtraction of a Shirley background utilising Scofield sensitivity factors with an energy dependence of -0.6

	XPS derived concentration at%					Pd/Au Ratio (XPS)
Catalyst	Au	Pd	Ti	O	C	
0.2Pd 0.8Au TiO_2	0.05	0.12	28.7	68.2	2.9	2.4
0.5Pd 0.5Au TiO_2	0.03	0.21	29.3	67.4	3.1	7
0.8Pd 0.2Au TiO_2	n/d	0.14	28.8	67.0	4.0	n/d

In order to be certain that the the Pd/Au ratio was indeed due to surface enrichment of Pd due to a core-shell structure, as opposed to a miscalculation during the catalyst preparation, bulk metal analysis was achieved by digesting the catalysts in aqua regia and quatifying the leachate by MP-AES. The results are given in table 2.

Table 2. Experimntally derived bulk analysis of the Au and Pd concentration on the bimetallic catalysts determined by MP-AES.

	Theoretical loading		Experimental loading	
Au:Pd Ratio	Au (wt%)	Pd (wt%)	Au (wt%)	Pd (wt%)
4:1	0.8	0.2	0.77%	0.20%
3:1	0.75	0.25	0.74%	0.25%
2:1	0.66	0.33	0.69%	0.37%
1:1	0.5	0.5	0.51%	0.49%
1:2	0.33	0.66	0.31%	0.63%
1:3	0.25	0.75	0.27%	0.74%
1:4	0.2	0.8	0.18%	0.77%

All catalysts were found to contain the theoretical loading of metal. It is clear from these results that the surface enrichment in the 0.5%Pd 0.5%Au TiO_2 catalyst is due to Pd enricement at the surface.

The increasing shell thickness observed in XPS can be explained when we consider the electron attenuation lengths for Au(4d) and Au(4f) electrons (*ca.* 1.4 and 1.6 nm respectively yielding an information depth of three times the attenuation length – *ca.* 4 and 5 nm respectively). Indeed, for the 0.8Au0.2Pd catalyst, both the Au(4d) signal is observable as is the Au(4f) signal, whilst no Au(4d) signal is observed for the 0.5Au0.5Pd catalyst and given the electron attenuation lengths discussed, the Au(4f) signal is still observable due to the greater information depth for these higher kinetic energy electrons. This information depth is clearly in line with the observed Pd shell thickness of *ca.* 5 nm shown in figures 4 and 5 surrounding the Au core, and the surface enrichment in Pd illustrated in table 1. Given these attenuation lengths and despite the presence of Au in the Pd shell, the majority of the Au signal originates from the gold core and the contribution from the surface Au species is minimal and exemplified by the absence of the Au(4d) signal in the core level spectra for the 0.5Au0.5Pd sample.

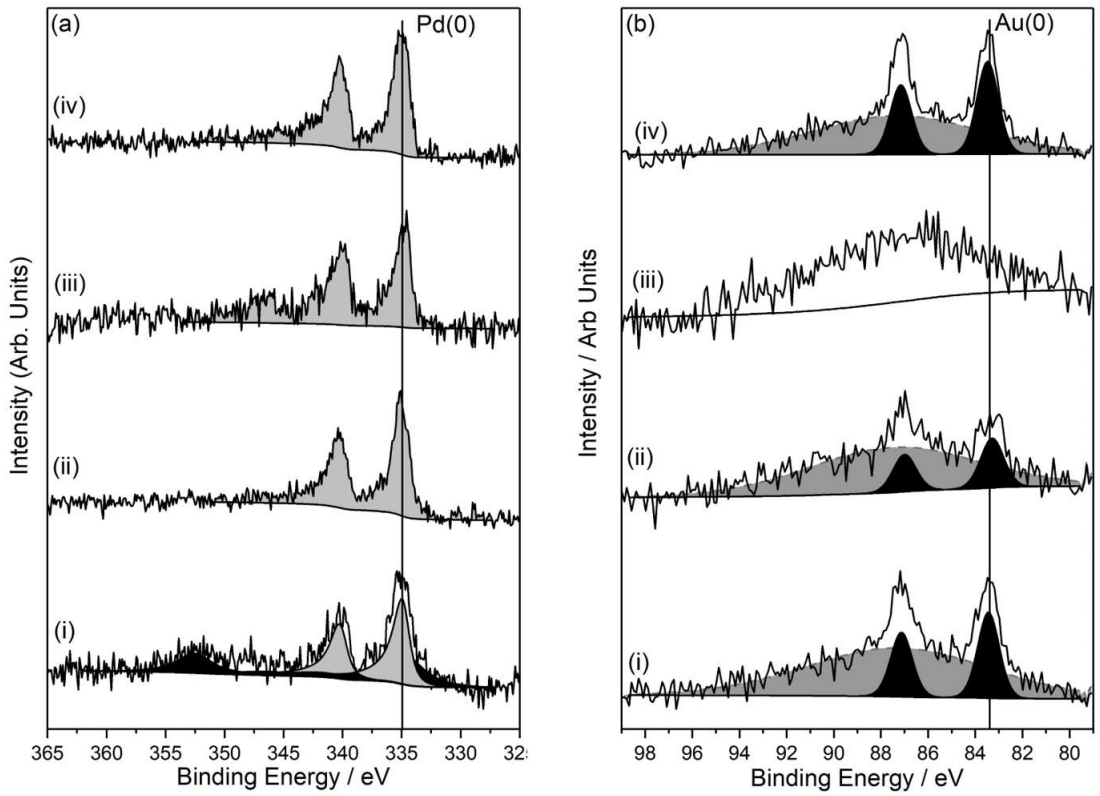

Figure 6. (a) Pd(3d)/Au(4d) core-level spectra for (i) 0.2Pd-0.8Au/TIO_2, (ii) 0.5Pd-0.5Au/TIO_2, (iii) 0.8Pd-0.2Au/TIO_2 and (iV) 1% Pd/TiO_2; grey and black shading indicate the Pd and Au components respectively. (b) Au(4f) core-level spectra for (i) 0.2Pd-0.8Au/TIO_2, (ii) 0.5Pd-0.5Au/TIO_2, (iii) 0.8Pd-0.2Au/TIO_2 and (iv) 1% Au/TiO_2; grey shading indicates the underlying titanium loss structure on which the Au signal (black shading) is superimposed.

The XPS and the STEM results are in agreement and seem to confirm that the catalyst are core shell in nature with a largely gold core and a bimetallic shell. When taken with the catalysts testing data, the model of the bimetallic composition of the shell aligns with the theoretical studies of Isihara *et al*.[36], who demonstrated that hydrogen peroxide destruction is more facile on a pure Pd surface, than one that is peppered with a few Au atoms, thus leading to a higher H_2O_2 yield on a bimetallic surface[28]. To the best of our knowledge this is the first example of a preparation method that can produce fully stable and reusable Pd@Au core shell structures and we have demonstrated their usefulness for the direct synthesis of hydrogen peroxide. The flexible, facile nature of the preparation technique means that it could be applied to different combinations of metals, potentially creating a range of interesting bimetallic core shell catalysts and this will form the basis of further studies.

Conclusions

1wt% supported Au, Pd and AuPd nanoalloy catalysts were prepared *via* the microwave assisted reduction of $PdCl_2$ and $HAuCl_4$, resulting in catalysts with high H_2O_2 synthesis activity. The bimetallic core-shell nanoparticles (evidenced by STEM, EDX and XPS characterisation) are formed under mild reaction conditions in a very short reactions time (150^{o}C in 15 min) compared to other methods that require either consecutive reduction methodologies (and litres of solvent) or high calcination temperatures (>400 ^{o}C). The activity of the catalyst is maintained after 4 reaction cycles, and the dispersion of the active phase is maintained when the loading of the catalyst is increased. This is the first time the preparation of stable, core-shell particles have been reported using microwave assisted reduction. The observation that these particles are core shell, without the need of a complicated synthesis or high thermal treatment and form in just 15 minutes presents an exciting opportunity for this experimental technique.

Acknowledgement

J.K.E would like to thank the German Catalysis network Unicat for the financial assistance and support that established this collaboration with P.S. JKE would like to thank Dr Samuel Pattisson, Cardiff Unviersity, for his assistance with timely MPAES. Q.H. would like to thank Professor Stephen J. Pennycook and National University of Singapore for the access of the aberration corrected microscope, and we thank Cardiff University for the funding.

References

1 N. Dimitratos, A. Villa, D. Wang, F. Porta, D. Su and L. Prati, *J. Catal.*, 2006, **244**, 113–121.

2 B. Katryniok, H. Kimura, E. Skrzyńska, J.-S. Girardon, P. Fongarland, M. Capron, R. Ducoulombier, N. Mimura, S. Paul and F. Dumeignil, *Green Chem.*, 2011, **13**, 1960.

3 N. Dimitratos, F. Porta, L. Prati and A. Villa, *Catal. Letters*, 2005, **99**, 181–185.

4 Y. Mizukoshi, T. Fujimoto, Y. Nagata, R. Oshima and Y. Maeda, *J. Phys. Chem. B*, 2000, **104**, 6028–6032.

5 J. Edwards, B. Solsona, P. Landon, A. Carley, A. Herzing, C. Kiely and G. Hutchings, *J. Catal.*, 2005, **236**, 69–79.

6 J. K. Edwards, A. F. Carley, A. A. Herzing, C. J. Kiely and G. J. Hutchings, *Faraday Discuss.*, 2008, **138**, 225–239.

7 P. J. Miedziak, Q. He, J. K. Edwards, S. H. Taylor, D. W. Knight, B. Tarbit, C. J. Kiely and G. J. Hutchings, *Catal. Today*, 2011, **163**, 47–54.

8 F. MOREAU, G. BOND and A. TAYLOR, *J. Catal.*, 2005, **231**, 105–114.

9 N. Dimitratos, F. Porta and L. Prati, *Appl. Catal. A Gen.*, 2005, **291**, 210–214.

10 J. A. Lopez-Sanchez, N. Dimitratos, P. Miedziak, E. Ntainjua, J. K. Edwards, D. Morgan, A. F. Carley, R. Tiruvalam, C. J. Kiely and G. J. Hutchings, *Phys. Chem. Chem. Phys.*, 2008, **10**, 1921.

11 Y. Ma, W. Li, E. C. Cho, Z. Li, T. Yu, J. Zeng, Z. Xie and Y. Xia, *ACS Nano*, 2010, **4**, 6725–6734.

12 J. K. Edwards, E. Ntainjua N, A. F. Carley, A. A. Herzing, C. J. Kiely and G. J. Hutchings, *Angew. Chemie Int. Ed.*, 2009, **48**, 8512–8515.

13 P. Strasser, S. Koh, T. Anniyev, J. Greeley, K. More, C. Yu, Z. Liu, S. Kaya, D.

Nordlund, H. Ogasawara, M. F. Toney and A. Nilsson, *Nat. Chem.*, 2010, **2**, 454–460.
14 D. I. Enache, *Science (80-.).*, 2006, **311**, 362–365.
15 R. C. Tiruvalam, J. C. Pritchard, N. Dimitratos, J. A. Lopez-Sanchez, J. K. Edwards, A. F. Carley, G. J. Hutchings and C. J. Kiely, *Faraday Discuss.*, 2011, **152**, 63.
16 H. Dong, Y.-C. Chen and C. Feldmann, *Green Chem.*, 2015, **17**, 4107–4132.
17 L. K. Kurihara, G. M. Chow and P. E. Schoen, *Nanostructured Mater.*, 1995, **5**, 607–613.
18 L. C. Varanda and M. Jafelicci, *J. Am. Chem. Soc.*, 2006, **128**, 11062–11066.
19 G. Viau, F. Fiévet-Vincent and F. Fiévet, *Solid State Ionics*, 1996, **84**, 259–270.
20 Y. Sun, Y. Yin, B. T. Mayers, T. Herricks and Y. Xia, *Chem. Mater.*, 2002, **14**, 4736–4745.
21 I. Pastoriza-Santos and L. M. Liz-Marzán, *Nano Lett.*, 2002, **2**, 903–905.
22 I. Pastoriza-Santos and L. M. Liz-Marzán, *Adv. Funct. Mater.*, 2009, **19**, 679–688.
23 M. Tsuji, M. Ogino, M. Matsunaga, N. Miyamae, R. Matsuo, M. Nishio and M. J. Alam, *Cryst. Growth Des.*, 2010, **10**, 4085–4090.
24 A. V. Gaikwad, P. Verschuren, S. Kinge, G. Rothenberg and E. Eiser, *Phys. Chem. Chem. Phys.*, 2008, **10**, 951–956.
25 R. T. Tom, A. S. Nair, N. Singh, M. Aslam, C. L. Nagendra, R. Philip, K. Vijayamohanan and T. Pradeep, *Langmuir*, 2003, **19**, 3439–3445.
26 S. Ayyappan, *Solid State Ionics*, 1996, **84**, 271–281.
27 I. Pastoriza-Santos and L. M. Liz-Marzán, *Langmuir*, 2002, **18**, 2888–2894.
28 N. Dahal, S. García, J. Zhou and S. M. Humphrey, *ACS Nano*, 2012, **6**, 9433–9446.
29 A. R. Vaino, *J. Org. Chem.*, 2000, **65**, 4210–4212.
30 D. G. Lee and U. A. Spitzer, *J. Org. Chem.*, 1970, **35**, 3589–3590.
31 G. Pfleiderer and H. J. Rledl, 1939.
32 P. Landon, P. J. Collier, A. F. Carley, D. Chadwick, A. J. Papworth, A. Burrows, C. J. Kiely and G. J. Hutchings, *Phys. Chem. Chem. Phys.*, 2003, **5**, 1917–1923.
33 B. E. Solsona, J. K. Edwards, P. Landon, A. F. Carley, A. Herzing, C. J. Kiely and G. J. Hutchings, *Chem. Mater.*, 2006, **18**, 2689–2695.
34 J. K. Edwards, B. Solsona, P. Landon, A. F. Carley, A. Herzing, M. Watanabe, C. J. Kiely and G. J. Hutchings, *J. Mater. Chem.*, 2005, **15**, 4595.
35 T. Ishihara, Y. Ohura, S. Yoshida, Y. Hata, H. Nishiguchi and Y. Takita, *Appl. Catal. A Gen.*, 2005, **291**, 215–221.
36 A. Staykov, T. Kamachi, T. Ishihara and K. Yoshizawa, *J. Phys. Chem. C*, 2008, **112**,

19501–19505.

37 J. Li, T. Ishihara and K. Yoshizawa, *J. Phys. Chem. C*, 2011, **115**, 25359–25367.

38 J. Pritchard, L. Kesavan, M. Piccinini, Q. He, R. Tiruvalam, N. Dimitratos, J. A. Lopez-Sanchez, A. F. Carley, J. K. Edwards, C. J. Kiely and G. J. Hutchings, *Langmuir*, 2010, **26**, 16568–16577.

39 J. C. Pritchard, Q. He, E. N. Ntainjua, M. Piccinini, J. K. Edwards, A. A. Herzing, A. F. Carley, J. A. Moulijn, C. J. Kiely and G. J. Hutchings, *Green Chem.*, 2010, **12**, 915.

40 J. K. Edwards, A. Thomas, B. E. Solsona, P. Landon, A. F. Carley and G. J. Hutchings, *Catal. Today*, 2007, **122**, 397–402.

41 J. K. Edwards, B. Solsona, E. N. N, A. F. Carley, A. A. Herzing, C. J. Kiely and G. J. Hutchings, *Science (80-.).*, 2009, **323**, 1037–1041.

42 J. A. Lopez-Sanchez, N. Dimitratos, P. Miedziak, E. Ntainjua, J. K. Edwards, D. Morgan, A. F. Carley, R. Tiruvalam, C. J. Kiely and G. J. Hutchings, *Phys. Chem. Chem. Phys.*, 2008, **10**, 1921.

43 J. K. Edwards, J. Pritchard, P. J. Miedziak, M. Piccinini, A. F. Carley, Q. He, C. J. Kiely and G. J. Hutchings, *Catal. Sci. Technol.*, 2014, **4**, 3244.

44 J. Pritchard, Cardiff University, 2012.

45 S. Song, Y. Wang and P. K. Shen, *J. Power Sources*, 2007, **170**, 46–49.

46 A. Villa, D. Wang, G. M. Veith, F. Vindigni and L. Prati, *Catal. Sci. Technol.*, 2013, **3**, 3036.

47 J. A. Lopez-Sanchez, N. Dimitratos, N. Glanville, L. Kesavan, C. Hammond, J. K. Edwards, A. F. Carley, C. J. Kiely and G. J. Hutchings, *Appl. Catal. A Gen.*, 2011, **391**, 400–406.

48 J. Pritchard, M. Piccinini, R. Tiruvalam, Q. He, N. Dimitratos, J. A. Lopez-Sanchez, D. J. Morgan, A. F. Carley, J. K. Edwards, C. J. Kiely and G. J. Hutchings, *Catal. Sci. Technol.*, 2013, **3**, 308–317.

49 A. Nirmala Grace and K. Pandian, *Mater. Chem. Phys.*, 2007, **104**, 191–198.

50 Z. Jiang, W. Zhang, L. Jin, X. Yang, F. Xu, J. Zhu and W. Huang, *J. Phys. Chem. C*, 2007, **111**, 12434–12439.

51 J. Radnik, C. Mohr and P. Claus, *Phys. Chem. Chem. Phys.*, 2003, **5**, 172–177.